Non-Orthogonal Pilot Designs with Collision Detection Capability For Grant-Free Access

Ayon Quayum,
Hlaing Minn
The University of Texas at Dallas
Richardson, TX, USA

Yuichi Kakishima,
Haralabos Papadopoulos
DOCOMO Innovations Inc.
Palo Alto, CA, USA

***Abstract*—In this paper we consider a densely deployed phantom cell system providing a low latency network for massive connectivity. Non-orthogonal pilot designs serve as a promising solution to support a large number of users but fast collision detection at the receiver is needed for low latency networks. Recently, a nice solution based on an on-off type non-orthogonal pilot design with collision detection capability has been proposed. It can serve more users than the orthogonal pilot design but at the cost of degraded channel estimation performance compared to the orthogonal optimum pilot design. We propose a new non-orthogonal pilot design with collision detection capability and improved channel estimation performance. An optimum threshold based detection criteria is developed. We further show that a dynamically calculated optimum threshold outperforms a fixed threshold based detection. Next, we investigated non-orthogonal pilot designs for fractional bandwidth allocation. We propose two new non-orthogonal pilot designs for physical resource block (PRB) based resource allocation. Both of the new designs support fast collision detection at the receiver. Performance evaluation results show that the proposed schemes provide equivalent or better channel estimation performance and support much more users than the orthogonal pilots defined in the current 4G standards.**

***Index Terms*—Small cell, channel estimation, non-orthogonal pilot, pilot collision, grant-free access**

I. Introduction

Growth of wireless traffic, densification of users and low latency requirements have created unique challenges for future wireless systems. 5G and other future standards are expected to provide support for high throughput, low latency and massive connectivity [1]. Different technologies are proposed and are being actively evaluated to achieve these goals. For example, small cell concept is used in different contexts to achieve high throughput. Dense deployment of remote radio head (RRH) is discussed in [2]. High density or "Big" phantom cell system provides another solution for increasing network capacity by splitting control and user (C/U) planes of the radio link [3].

User-centric ultra-dense network is discussed in [4]. In this regard, a user-centric no-cell (UCNC) system in conjunction with grant-free non-orthogonal uplink (UL) access is demonstrated in [5]. This system supports massive connectivity with low latency and overhead. For grant-free uplink access, it is essential for base station (BS) to obtain channel state information (CSI) from initial transmission. This could be achieved by using carefully designed embedded pilot sequences.

In existing systems, orthogonal pilot sequences are re-used based on spatial separation to minimize pilot contamination [6]. This translates to poor efficiency in the spatial reuse of pilot resources. Another approach is to create a large pool of orthogonal pilot sequences and let users choose them randomly [5]. However, large overhead is needed for a sufficient number of orthogonal pilot sequences to minimize pilot collision probabilities.

One way to reduce inefficiency and large overhead is to use non-orthogonal pilot sequences with collision detection capabilities. A nice solution based on on-off type non-orthogonal pilot codes has been proposed in [7]. This scheme uses L non-zero pilot dimensions and L' null pilot dimensions to create non-orthogonal pilot sequences from a total of $(L + L')$ pilot resources. More than L non-zero pilot dimensions indicates a collision at the receiver. Further analysis shows that sectorization could increase area multiplexing gain by resolving more collision-free users per unit area [8] [9]. A similar non-orthogonal pilot design has been used with compressed sensing channel estimation in [10].

The existing non-orthogonal pilot code designs are not optimized for channel estimation performance. As a result, they suffer from degraded channel estimation performance. Another shortcoming is the vastly different channel estimation performances for different pilot sequences which makes this design inherently unfair to different users. In this paper, by incorporating both collision detection capability and channel estimation performance in the design, we develop novel non-orthogonal pilot designs for both full and fractional bandwidth allocations. The proposed designs overcome the shortcomings of the existing designs and provide substantially better channel estimation performance and fairness to users.

II. System Model

We consider a "Big" phantom cell system with dense deployment of small cells. Such a system will face severe uplink pilot contamination with growing traffic. To alleviate this problem, we consider grant-free uplink access and fast user detection for our system. Time-Division Duplexing (TDD) and uplink-downlink (UL-DL) channel reciprocity is assumed. This allows non-orthogonal pilot sequences or codes to be used for acquisition of CSI at the transmitter. Pilot codes are designed with fast collision detection capability. A user can select a non-orthogonal pilot code randomly from a set of pilot codes. BS should be able to detect a collision when more than

978-1-5386-3180-5/18/$31.00

one non-orthogonal pilot codes from the same pilot codes set are received.

We use an orthogonal frequecy division mltiplexing (OFDM) system with discrete Fourier transform (DFT) size N. For user i, let us define the frequency domain pilot vector as $\boldsymbol{c}_i$ of length N and the time domain pilot vector as $\boldsymbol{s}_i$ of length N. The channel impulse response (CIR) vector $\boldsymbol{h}_i$ consists of L sample-spaced channel taps (we assume timing errors or different propagation delays are already absorbed into the CIR). Cyclic prefix length $L_{\rm CP}$ ($\geq L$) is used. Define N-point unitary DFT matrix $\boldsymbol{F} = [\boldsymbol{f}_0, \boldsymbol{f}_1, \ldots, \boldsymbol{f}_{N-1}]$ and $\boldsymbol{F}_L = [\boldsymbol{f}_0, \boldsymbol{f}_1, \ldots, \boldsymbol{f}_{L-1}]$ where $\boldsymbol{f}_k = [1, e^{-j2\pi k/N}, \ldots, e^{-j2\pi k(N-1)/N}]^T/\sqrt{N}$. The received time domain signal vector for a single OFDM symbol from M users is given by [11]

$$\boldsymbol{y} = \sum_{i=1}^{M} \boldsymbol{S}_i \boldsymbol{h}_i + \boldsymbol{n}, \tag{1}$$

where $\boldsymbol{y} = [y_0,\ y_1,\ \ldots,\ y_{N-1}]^T$, $\boldsymbol{S_i} = \sqrt{N}\boldsymbol{F}^H \boldsymbol{C_i} \boldsymbol{F}_L$, $\boldsymbol{C_i} = \text{diag}\{\boldsymbol{c_i}\}$ and $\boldsymbol{n}$ is zero-mean complex Gaussian noise vector of length N with covariance matrix $\sigma_n^2 \boldsymbol{I}$. Assuming $(\boldsymbol{S}_i^H \boldsymbol{S}_i)$ is full rank, the least-square (LS) CIR estimation for user i is given by [12]

$$\hat{\boldsymbol{h}}_i = \left(\boldsymbol{S}_i^H \boldsymbol{S}_i\right)^{-1} \boldsymbol{S}_i^H \boldsymbol{y}. \tag{2}$$

For orthogonal pilot designs, optimality is achieved when

$$\begin{aligned} \boldsymbol{S}_i^H \boldsymbol{S}_i &= E_{\rm av} \boldsymbol{I}, \quad \forall i, \\ \boldsymbol{S}_i^H \boldsymbol{S}_j &= \boldsymbol{0}, \quad \forall i \neq j \end{aligned} \tag{3}$$

where $E_{\rm av}$ is average OFDM symbol energy [13]. After satisfying these conditions, the mean square error (MSE) for channel estimation is given by $\sigma_n^2 \text{tr}\big(\boldsymbol{S}_i^H \boldsymbol{S}_i\big)^{-1} = L\sigma_n^2/E_{\rm av}$. Several optimum orthogonal pilot designs have been discussed in [13]. However, using orthogonal pilot codes is incapable of supporting a large number of users. In this paper, we will develop non-orthogonal pilot codes based on frequency division multiplexing (FDM) type orthogonal pilot sets with cyclically equi-spaced pilot tones.

We observe some shortcomings of the existing non-orthogonal pilot design [7] in the literature. First, its average channel estimation performance is substantially degraded compared to the performance achieved by the optimum orthogonal pilot design. Second, different pilot codes may have vastly unequal channel estimation performances.

To illustrate these shortcomings, let us consider an example system with DFT size $N = 128$ and $L = 8$ sample-spaced channel taps. Fig. 1 shows channel estimation MSEs for different non-orthogonal pilot codes of the existing design for 0 dB SNR. The MSEs for different pilot codes vary substantially, which translates into unfair quality of service provisioning to different users. This also highlights the need of efficient non-orthogonal pilot designs with good channel estimation performance and capability to support a large number of users with low latency.

III. Proposed Non-orthogonal Pilot Design

To overcome limitations of the existing pilot design for grant-free access, we propose a novel non-orthogonal pilot design satisfying the following criteria:

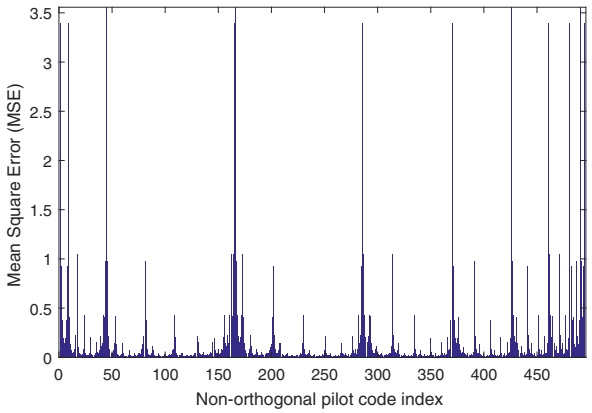

Fig. 1. Channel estimation performance of different non-orthogonal pilot codes from the existing design (SNR=0 dB)

- Channel estimation performance should match closely with optimum orthogonal pilot design.
- Different pilot sequences should have similar channel estimation performances to ensure fairness.
- Receiver should be able to detect collision when more than one non-orthogonal pilot codes are present.
- Pilot design should support a large number of non-orthogonal users.

The new pilot design is based on the FDM type orthogonal pilot tone index sets described in [13] for estimating L sample-spaced channel taps. In this orthogonal pilot design, each pilot set contains L cyclically equi-spaced equal energy pilot tones. Our non-orthogonal pilot design is described as follows.

1) For DFT size N, we define the total number of orthogonal sets $D = N/L$ and their pilot tone index set $\{J_k : k = 0, 1 \ldots D-1\}$ according to the FDM design in [13] where $J_k = J_{k-1} + 1$. The set J_0 which contains indexes 0 and $N/2$ (i.e., the DC tone and the band-edge tone which are typically set to be null tones), is treated separately. Define the total number of remaining pilot index sets as $D' = D - 1$.
2) Define $J_{k,a} \triangleq \{J_k[i] : i = 1, 3, 5, \ldots\},\ k = 1, 2 \ldots D'$ and $J_{k,b} \triangleq \{J_k[i] : i = 2, 4, 6, \ldots\},\ k = 1, 2 \ldots D'$. Also define $\tilde{D} = \left\lfloor \frac{D'}{3} \right\rfloor$. Then, each of the $2\tilde{D}$ pilot groups defined by their pilot tone index sets $\{\tilde{J}_k\}$ is constructed by combining two contiguous orthogonal pilot tone index sets in the following way:
$\tilde{J}_1 = J_1 \cup J_{2,a}, \quad \tilde{J}_2 = J_3 \cup J_{2,b}$
$\tilde{J}_3 = J_4 \cup J_{5,a}, \quad \tilde{J}_4 = J_6 \cup J_{5,b}$
$\ldots\ldots\ldots$
$\tilde{J}_{2(\tilde{D}-1)+1} = J_{3(\tilde{D}-1)+1} \cup J_{3(\tilde{D}-1)+2,a}$
$\tilde{J}_{2(\tilde{D}-1)+2} = J_{3(\tilde{D}-1)+3} \cup J_{3(\tilde{D}-1)+2,b}$
3) Each group's pilot tone index set $\tilde{J}_k$ contains $L/2$ pairs of pilot tones where the two tones in each pair are adjacent and $L/2$ unpaired pilot tones. Each pair is composed of one non-zero pilot tone and one null pilot tone while unpaired

ones are non-zero pilots tones. All the L non-zero pilot tones within $\tilde{J}_k$ have the same amplitude a. Selecting $L/2$ non-zero pilots from $L/2$ pairs yields $2^{L/2}$ non-orthogonal pilot codes within the pilot group defined by $\tilde{J}_k$.

4) Non-zero tones from J_0 and $\left\{J_k : k = 3\tilde{D}+1 \ldots D'\right\}$ can be distributed to adjacent $\tilde{J}_k$ sets as evenly as possible. For example, define $(L-2)$ non-zero tones of J_0 as $J_0' = \left\{J_0 \backslash \left\{0, \frac{N}{2}\right\}\right\}$. Then, we can add $J_{0,a}'$ to $\tilde{J}_1$ and $J_{0,b}'$ to $\tilde{J}_{\tilde{D}}$. In this case, the pilot groups defined by $\tilde{J}_1$ and $\tilde{J}_{\tilde{D}}$ have 2^{L-1} non-orthogonal pilot codes in each group.

Channel estimation MSE of the proposed pilot code k from the group based on $\tilde{J}_i$, if without collision within the group, is given by $\sigma_n^2 \mathrm{tr}(\boldsymbol{S}_k^H \boldsymbol{S}_k)^{-1}$. Due to the choice of adjacent tones for pilot pairs, some pilot codes will maintain $\boldsymbol{S}_k^H \boldsymbol{S}_k = E_{\mathrm{av}} \boldsymbol{I}$ while the others will have $\boldsymbol{S}_k^H \boldsymbol{S}_k \approx E_{\mathrm{av}} \boldsymbol{I}$. Note that phases of the non-zero pilot sequence do not affect MSE and hence they can be designed to yield low peak to average power ratio (PAPR) of the time domain signal.

To illustrate our non-orthogonal pilot design, let us consider a system with DFT size of $N = 128$ and $L = 8$ sample-spaced channel taps. Each FDM orthogonal pilot set consists of $L = 8$ pilot tones. If we exclude J_0 due to practical setting of null tones at index 0 and $N/2$, the total number of orthogonal pilot sets is $D = 15$. The proposed non-orthogonal pilot tone index sets are:

$\tilde{J}_1 = [(1\ 2)\ 17\ (33\ 34)\ 49\ (65\ 66)\ 81\ (97\ 98)\ 113]$

$\tilde{J}_2 = [3\ (18\ 19)\ 35\ (50\ 51)\ 67\ (82\ 83)\ 99\ (114\ 115)]$

. . . . . .

$\tilde{J}_{10} = [15\ (30\ 31)\ 47\ (62\ 63)\ 79\ (94\ 95)\ 111\ (126\ 127)]$

where the indexes of pilot pairs are shown in the bracket. There are 10 orthogonal pilot groups defined by $\{\tilde{J}_1, \ldots, \tilde{J}_{10}\}$ and each group has $2^4 = 16$ non-orthogonal pilot codes since there are 4 pairs of adjacent pilot tones. Each pilot code has 4 null pilot tones (one from each pilot tone pair) and 8 non-zero pilot tones with amplitude a on the remaining tones. For example, within the group $\tilde{J}_1$, the non-zero pilot tone indexes of the first four non-orthogonal pilot codes are $\{1, 33, 65, 97, 17, 49, 81, 113\}$, $\{2, 33, 65, 97, 17, 49, 81, 113\}$, $\{1, 34, 65, 97, 17, 49, 81, 113\}$, and $\{2, 34, 65, 97, 17, 49, 81, 113\}$. Fig. 2 shows an example of designing non-orthogonal pilot groups from orthogonal pilot sets. Table I provides details about the pilot resource amount and the number of users supported by different pilot designs.

In existing orthogonal pilot design, there are several orthogonal pilot sets where each set can support only one pilot code. Our new pilot design has smaller number of orthogonal pilot sets while each set can support multiple pilot codes. Different orthogonal pilot sets could be used for different antennas or different user groups. So the new pilot design is easily applicable for multiple antenna systems.

Fig. 3 compares channel estimation performance of the proposed non-orthogonal pilot codes with that of orthogonal optimum design and the existing non-orthogonal design. The proposed design provides an improvement of around 15 dB

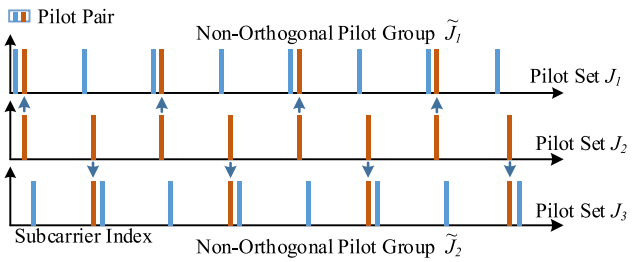

Fig. 2. Design of non-orthogonal pilot codes from orthogonal pilot sets

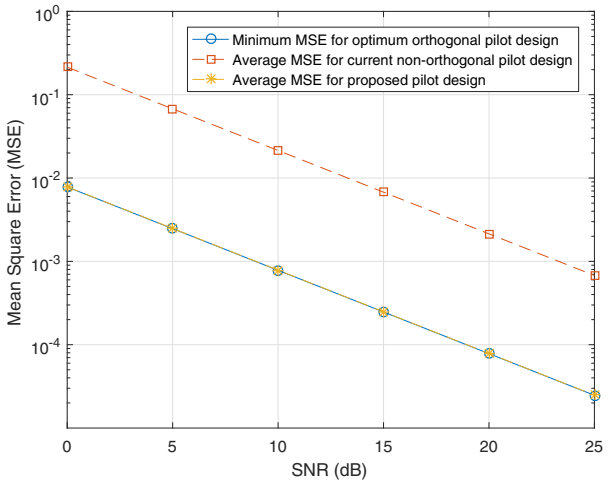

Fig. 3. Channel estimation performance comparison among different pilot designs in a system with $N = 128$ subcarriers and $L = 8$ channel taps

compared to the existing non-orthogonal design and its performance closely matches that of orthogonal design.

Fig. 4 shows the channel estimation MSE for different non-orthogonal pilot codes within a pilot group of the proposed design. By comparing the corresponding results of the existing design in Fig. 1, we can observe that the MSE performances for different codes are essentially the same for the proposed design while they vary substantially for the existing design. Thus, the proposed non-orthogonal pilot design offers fairness to different users.

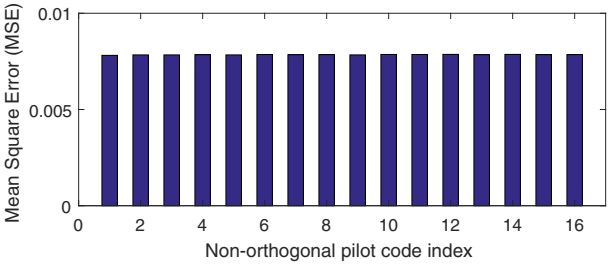

Fig. 4. Channel estimation performance of the proposed non-orthogonal pilot codes within a pilot group (SNR=0 dB)

IV. Threshold-Based Pilot Detection

At the receiver, the energy of each pilot tone in a pilot index set $\tilde{J}_k$ is compared with a predefined detection threshold. The receiver detects a non-zero pilot tone if the received energy

on that tone exceeds the detection threshold. A single user is detected if exactly L non-zero pilot tones are detected and the non-zero tones correspond to a valid pilot index set $\tilde{J}_k$. A collision is detected if more than L non-zero pilot tones are detected. Otherwise, no user is detected. Next, we will consider the threshold-based pilot detection performance. We will define two performance metrics: probability of single user detection (P_{SUD}) and probability of collision detection (P_{CD}). P_{SUD} is defined as the probability of detecting the pilot correctly when only one user transmits the pilot code and P_{CD} is defined as the probability of detecting a collision when more than one user transmit non-orthogonal pilot codes within a pilot codes group.

A. Probability of Single User Detection (P_{SUD})

Non-zero pilot tones are detected based on the received energy levels of the pilot subcarriers. For the threshold based detection, the energy of each of the possible pilot tones in a pilot codes set is compared to a predefined threshold value to determine an active or null pilot. Let us consider the received energies of a pilot code consisting of L active pilot tones of indexes $(q_1, q_2 ... q_L)$ and L' null tones of indexes $(q'_1, q'_2 ... q'_{L'})$. Also define the ratio (L'/L) as γ, the transmit pilot power on each non-zero pilot tone as a^2 and noise power per tone as N_0. Frequency domain received signal is $\boldsymbol{Y} = \boldsymbol{Fy}$ where $\boldsymbol{Y} = [Y_0\ Y_1\ \ldots\ Y_{N-1}]^T$. For a Rayleigh fading channel, the average received power on a pilot subcarrier is given by

$$E\left[|Y_k|^2\right] = \begin{cases} a^2 + N_0, & k \in q \\ N_0, & k \in q' \end{cases} \tag{4}$$

The SNR is defined as $\mathrm{SNR} = \frac{E_{\mathrm{av}}}{NN_0}$ where $E_{\mathrm{av}} = La^2$.

Let the detection threshold be τ. Then, P_{SUD} is given by

$$P_{\mathrm{SUD}} = P\left[\left(\cap_{i\in\{q_l\}}\left(|Y_i|^2 > \tau\right)\right) \cap \left(\cap_{j\in\{q'_l\}}\left(|Y_j|^2 < \tau\right)\right)\right]$$

Assuming all received pilot tones are independent, we can compute the probability of single user detection as

$$\begin{aligned} P_{\mathrm{SUD}} &= \Big[\prod_{i\in\{q_l\}} P\left(|Y_i|^2 > \tau\right)\Big]\Big[\prod_{j\in\{q'_l\}} P\left(|Y_j|^2 < \tau\right)\Big] \\ &= \left[1 - F\left(\frac{2\tau}{a^2+N_0}\right)\right]^L \left[F\left(\frac{2\tau}{N_0}\right)\right]^{L'} \end{aligned} \tag{5}$$

where $F(x)$ is an exponential cumulative distribution function given by

$$F(x) = 1 - e^{-\frac{x}{2}}. \tag{6}$$

Substituting (6) in (5) and using $L' = \gamma L$, we get

$$P_{\mathrm{SUD}} = \left[e^{-\left(\frac{2\tau}{2(a^2+N_0)}\right)}\right]^L \left[1 - e^{-\left(\frac{2\tau}{2N_0}\right)}\right]^{\gamma L}. \tag{7}$$

Now, we can find the optimum detection threshold by maximizing P_{SUD} as follows. First, we take the first derivative of P_{SUD} and equate it to zero as

$$\frac{d}{d\tau}\left(\left[e^{-\left(\frac{\tau}{(a^2+N_0)}\right)}\right]^L \left[1 - e^{-\left(\frac{\tau}{N_0}\right)}\right]^{\gamma L}\right) = 0. \tag{8}$$

By solving (8), we obtain the optimum detection threshold as

$$\tau_{\mathrm{opt}} = -N_0 \ln\left(\frac{L}{\gamma N\ \mathrm{SNR} + L(1+\gamma)}\right). \tag{9}$$

Equation (9) shows that the optimum value of the detection threshold depends on the SNR value. The threshold can be set based on the targeted SNR of the considered application, which we call a fixed threshold setting.

Alternatively, we can calculate τ_{opt} based on the instantaneous SNR estimate and use it as a detection threshold. This dynamic threshold setting improves the detection performance compared to the fixed threshold setting. To illustrate the performance gain from the dynamic detection threshold, we consider the previous example with DFT size 128 and 8 non-zero pilot tones per pilot group. Fig. 5 shows P_{SUD} using a fixed threshold ($\tau = 1$) and a dynamic threshold for different SNRs. The fixed threshold is only optimum for a certain SNR value. In all other cases, the dynamic threshold provides performance gain.

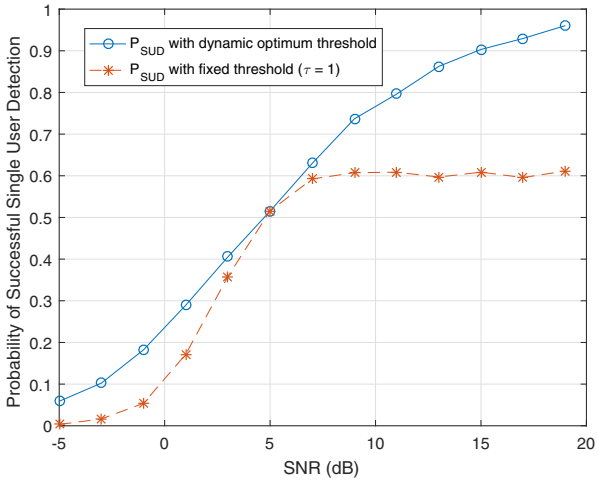

Fig. 5. Single user detection performance for the dynamic versus fixed detection threshold settings

B. Probability of Collision Detection (P_{CD})

Another important performance metric is the probability of collision detection P_{CD}. We use the previous example to illustrate the effect of the detection threshold for P_{CD}. We use scenarios with two non-orthogonal pilot users within a pilot group in Fig. 6(a) and three users within a pilot group in Fig. 6(b). In our simulation, all users have the same SNR. We plot P_{SUD} against P_{CD} for 10 dB SNR. In the plot each point corresponds to a different detection threshold value. Fig. 6 shows that the optimum threshold for P_{SUD} also provides high probability of collision detection. So we can conclude that the optimum detection threshold for the single user detection performance is also a good choice for the collision detection performance.

V. Design for Fractional Bandwidth Allocation

Now we will develop two different pilot schemes for fractional bandwidth (BW) allocation, denoted as Scheme A and B. Both of them use Physical Resource Block (PRB) similar to what is defined in 4G standards for 3GPP Long Term Evolution (LTE) downlink reference signal (RS) as a resource allocation unit. Each PRB consists of 12 subcarriers and 7 symbols (1 time slot). A single symbol and one subcarrier creates time-frequency resource element (RE). We consider

TABLE I. Pilot resource amount and the number of supported users for different pilot designs

BW allocation	Design	# of pilot REs per pilot group	# of orthogonal pilot groups	# of users supported per pilot group	total # of users supported
Full BW allocation	Orthogonal	8	15	1	15
	Proposed non-orthogonal	12	10	16	160
Fractional BW allocation	Orthogonal (4G standards)	16	1	1	1
	Proposed non-orthogonal Scheme A ($r = 2$)	20	1	16	16
	Proposed non-orthogonal Scheme B	16	1	128	128

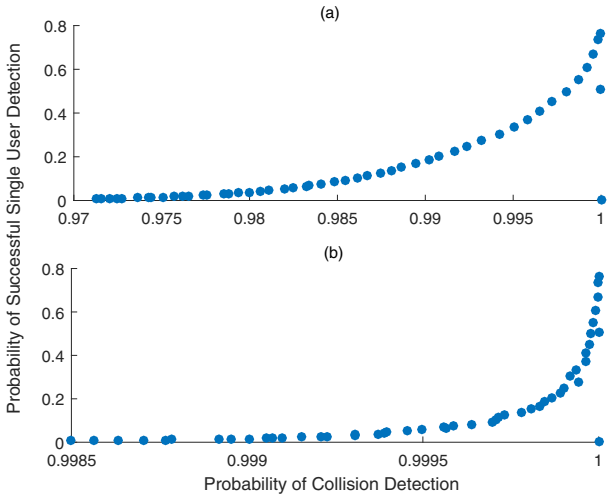

Fig. 6. Single user detection performance versus collision detection performance for different detection threshold values. a) 2 users per pilot group, b) 3 users per pilot group.

few REs to be dedicated for pilot sequences in each PRB. Other REs will be used for data transmission. For both of the schemes, we will use the concept of pilot pairs similar to our non-orthogonal pilot design in Section III.

A. Scheme A

In LTE standards, two pilot tones are used in each of first and third from the last OFDM symbol of each time slot. The two pilot tones in one OFDM symbol is evenly distributed in a PRB with 6 subcarriers spacing between them. We propose one additional pilot tone in the first OFDM symbol of every r-th PRB. The additional pilot RE will be placed adjacent to one of the existing pilot subcarriers. These two adjacent pilot tones will create a pilot pair. To create non-orthogonal pilot codes, we will use one non-zero pilot and one null pilot from each pilot pair allocated in a pilot set. If the number of PRBs allocated with additional pilots is S, the pilot set can have up to 2^S non-orthogonal pilot codes.

B. Scheme B

Scheme B is suitable when the allocated PRBs are contiguous in frequency. We use two pilots tones in each of first and third from the last OFDM symbol of each time slot. We use first and last subcarrier in each of these OFDM symbols as pilot tones. First subcarrier of the first allocated PRB and last subcarrier of the last allocated PRB are always used as non-zero pilots. For the remaining PRBs, last and first pilots of adjacent PRBs will create a pilot pair which are contiguous in frequency. We use one non-zero pilot from each available pilot pair to create non-orthogonal pilot codes. A pilot set has $(T + 1)$ non zero pilots and can support up to $2^{(T-1)}$ non-orthogonal pilot codes where T is the total number of allocated PRBs.

Fig. 7 shows pilot locations for Scheme A and Scheme B where adjacent pilot tones are used as pilot pairs.

Table I summarizes the numbers of users supported and pilot resources used by different pilot designs.

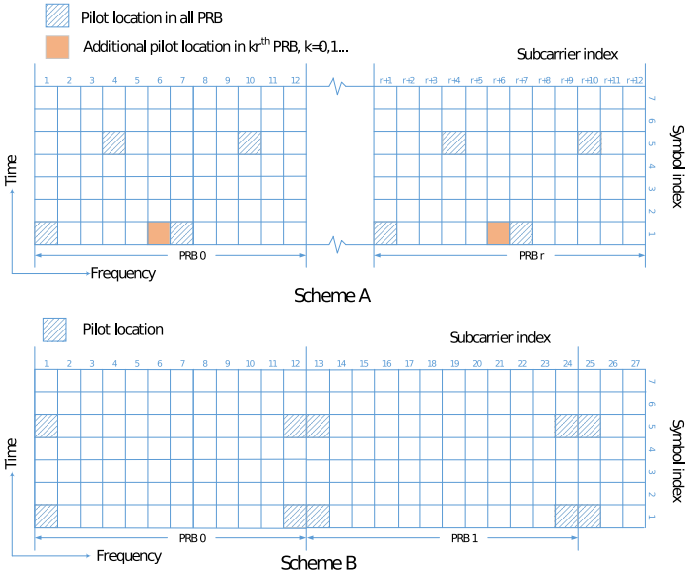

Fig. 7. Proposed pilot Scheme A and Scheme B for the fractional bandwidth allocation

C. Channel Estimation Performance for Fractional Bandwidth

To evaluate channel estimation performance for these schemes, let us assume R consecutive tones at indexes $(r_1, r_2 \dots r_R)$ are allocated to each user. We consider the channel to be time-invariant for the span of one PRB. Thus, we will use just one OFDM symbol for channel estimation. Let $\boldsymbol{X_P} = \text{diag}\{c_{q_1}, c_{q_2} \dots c_{q_P}\}$ be a diagonal matrix with non-zero pilot tones as its diagonal elements and $\boldsymbol{H}_P = [H_{q_1} H_{q_2} \dots H_{q_P}]^T$ be the channel frequency response (CFR)

of the pilot subcarriers. Then the received frequency domain pilot vector for the considered pilot code is given by

$$\boldsymbol{Y}_P = \boldsymbol{X}_P \boldsymbol{H}_P + \boldsymbol{N}_P \tag{10}$$

where $\boldsymbol{N}_P$ is the noise vector on pilot subcarriers with covariance $\sigma_n^2 \boldsymbol{I}$. For L sample-spaced channel taps, the estimate of CFR for allocated bandwidth of R tones is given by

$$\hat{\boldsymbol{H}}_R = \boldsymbol{F}_R \left(\boldsymbol{F}_{PL}^H \boldsymbol{F}_{PL} \right)^{-1} \boldsymbol{F}_{PL}^H \hat{\boldsymbol{H}}_P \tag{11}$$

where

$\hat{\boldsymbol{H}}_R$ =Estimate of CFR for R tones

$\hat{\boldsymbol{H}}_P = \boldsymbol{X}_P^{-1} \boldsymbol{Y}_P$, LS estimate of CFR for P pilot tones

$\boldsymbol{F}_R$ =First L columns and R rows corresponding to tone indexes $(r_1, \ldots, r_R)$ of DFT matrix $\boldsymbol{F}$

$\boldsymbol{F}_{PL}$ =First L columns and P rows corresponding to pilot tone indexes $(q_1, \ldots, q_P)$ of DFT matrix $\boldsymbol{F}$

The corresponding MSE is given by

$$E\left[||\hat{\boldsymbol{H}}_R - \boldsymbol{H}_R||^2 \right] = \sigma_n^2 \, \mathrm{tr}\left(\boldsymbol{A} \left(\boldsymbol{X}_P^H \boldsymbol{X}_P \right)^{-1} \boldsymbol{A}^H \right) \tag{12}$$

where $\boldsymbol{A} = \boldsymbol{F}_R \left(\boldsymbol{F}_{PL}^H \boldsymbol{F}_{PL} \right)^{-1} \boldsymbol{F}_{PL}^H$.

To compare the performance of different schemes, let us consider an example of 8 consecutive PRB allocation per user. We will use DFT size of 512 and 8 sample-spaced channel taps. Original orthogonal pilot scheme has a total of 16 non-zero pilots within the allocated bandwidth. For scheme A we will use $r = 2$ (i.e., add a new pilot RE in every other PRBs). This makes a total of 20 pilot REs and 16 non-zero pilot REs available to each user. Scheme B uses a total of 16 pilot REs and 9 non-zero pilot REs for each pilot set. Scheme A can support 16 users and Scheme B can support up to 128 users with non-orthogonal pilot codes while the original scheme can support only one user. See Table I for comparison. Fig. 8 shows the channel estimation performance of different pilot designs for the fractional bandwidth allocation. Scheme A and the orthogonal allocation scheme has comparable performance. Scheme B performs better compared to other schemes as its use of both band edge subcarriers for non-zero pilots yields better channel interpolation.

VI. Conclusions

In this paper, we have developed a novel non-orthogonal pilot design that outperforms the existing design in channel estimation performance, supports collision detection at the receiver and could accommodate a large number of users through non-orthogonal pilot codes. Also we have developed an optimum threshold based pilot detection scheme. Our simulation shows that when the detection threshold is dynamically set, it could lead to better performance over a broader SNR range. We have also presented two non-orthogonal pilot designs for systems using a fractional bandwidth allocation. Both of these schemes provide similar or better channel estimation performances compared to the existing design while supporting a higher number of non-orthogonal users and providing collision detection capability.

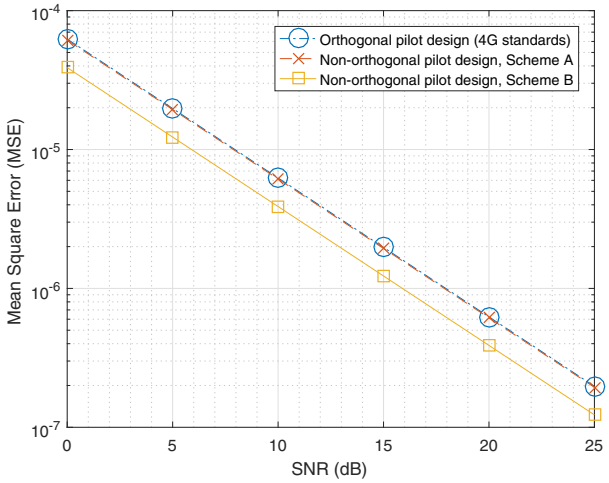

Fig. 8. Channel estimation performance for different pilot designs in the fractional bandwidth allocation

References

[1] C. Bockelmann, N. Pratas, H. Nikopour, K. Au, T. Svensson, C. Stefanovic, P. Popovski, and A. Dekorsy, "Massive machine-type communications in 5G: Physical and MAC-layer solutions," *IEEE Commun. Mag.*, vol. 54, no. 9, pp. 59–65, 2016.

[2] M. Peng, S. Yan, and H. V. Poor, "Ergodic capacity analysis of remote radio head associations in cloud radio access networks," *IEEE Wireless Commun. Lett.*, vol. 3, no. 4, pp. 365–368, 2014.

[3] H. Ishii, Y. Kishiyama, and H. Takahashi, "A novel architecture for LTE-B: C-plane/U-plane split and phantom cell concept," in *Globecom Workshops (GC Wkshps), 2012*. IEEE, 2012, pp. 624–630.

[4] S. Chen, F. Qin, B. Hu, X. Li, and Z. Chen, "User-centric ultra-dense networks for 5G: challenges, methodologies, and directions," *IEEE Wireless Commun.*, vol. 23, no. 2, pp. 78–85, 2016.

[5] J. Zhang, L. Lu, Y. Sun, Y. Chen, J. Liang, J. Liu, H. Yang, S. Xing, Y. Wu, J. Ma *et al.*, "PoC of SCMA-based uplink grant-free transmission in UCNC for 5G," *IEEE J. Sel. Areas Commun.*, vol. 35, no. 6, pp. 1353–1362, 2017.

[6] T. L. Marzetta, "Noncooperative cellular wireless with unlimited numbers of base station antennas," *IEEE Trans. Wireless Commun.*, vol. 9, no. 11, pp. 3590–3600, 2010.

[7] O. Y. Bursalioglu, C. Wang, H. Papadopoulos, and G. Caire, "RRH based massive MIMO with "on the fly" pilot contamination control," in *IEEE Intl. Conf. Commun. (ICC)*, 2016, pp. 1–7.

[8] O. Bursalioglu, C. Wang, H. Papadopoulos, and G. Caire, "A novel alternative to cloud RAN for throughput densification: Coded pilots and fast user-packet scheduling at remote radio heads," in *Fiftieth Asilomar Conference on Signals, Systems and Computers*. IEEE, 2016, pp. 3–10.

[9] Z. Li, N. Rupasinghe, O. Y. Bursalioglu, C. Wang, H. Papadopoulos, and G. Caire, "Directional training and fast sector-based processing schemes for mmWave channels," in *IEEE Intl. Conf. Commun. (ICC)*, 2017, pp. 1–7.

[10] W. C. Ao, C. Wang, O. Y. Bursalioglu, and H. Papadopoulos, "Compressed sensing-based pilot assignment and reuse for mobile UEs in mmWave cellular systems," in *IEEE Intl. Conf. Commun. (ICC)*, 2016, pp. 1–7.

[11] Y. Li, H. Minn, N. Al-Dhahir, and A. R. Calderbank, "Pilot designs for consistent frequency-offset estimation in OFDM systems," *IEEE Trans. Commun.*, vol. 55, no. 5, pp. 864–877, 2007.

[12] L. S. Louis, "Statistical signal processing: detection, estimation, and time series analysis," *Addision-Wesley Publishing company*, 1991.

[13] H. Minn and N. Al-Dhahir, "Optimal training signals for MIMO OFDM channel estimation," *IEEE Trans. Wireless Commun.*, vol. 5, no. 5, pp. 1158–1168, 2006.